Meteoritics & Planetary Science 37, 1223–1231 (2002)
Available online at http://www.uark.edu/meteor

Source and maintenance of the argon atmospheres of Mercury and the Moon

R. M. KILLEN

University of Maryland, Department of Astronomy, College Park, Maryland 20742, USA
Author's e-mail address: rkillen@astro.umd.edu

(Received 2002 January 11; accepted in revised form 2002 May 29)
(Presented at the Workshop on Mercury, The Field Museum, Chicago, Illinois, 2001 October 4–5)

Abstract–We propose that argon-40 measured in the lunar atmosphere and that in Mercury's atmosphere is due to current diffusion into connected pore space within the crust. Higher temperatures at Mercury, along with more rapid loss from the atmosphere, will lead to a similar or smaller column abundance of argon at Mercury than at the Moon, given the same crustal abundance of potassium. Because the noble gas abundance in the mercurian atmosphere represents current effusion, it is a direct measure of the crustal potassium abundance. We assume a fractal distribution of distance to a connected pore space, with the shortest distance increasing with depth. Given this "rock size" distribution, we show that the diffusive flux is not a unique function of temperature. Even though the diffusion coefficient is an exponential function of temperature, the flux to the surface is fairly insensitive to the temperature.

INTRODUCTION

We reconsider the source and loss processes for the argon atmospheres of Mercury and the Moon in order to investigate what these atmospheres tell us about the structure and composition of the megaregolith. Argon is especially important because it does not engage in chemistry. In order to interpret measurements of argon in Mercury's atmosphere, we must have a model including sources from the interior and loss from the atmosphere. Our model will be trained on the Moon, where data from *in situ* measurements are available from instruments left on the surface by the Apollo 17 astronauts. We consider diffusion of radiogenic argon from the regolith and megaregoliths of Mercury and the Moon to the atmosphere, and its subsequent escape *via* ionization and entrainment in the solar wind. We will not consider diffusion in the atmosphere itself, leading to a redistribution of argon in the atmosphere as considered by Hodges (1975), nor do we consider the possibility of argon trapping in the polar regions, previously considered by Hodges (1980). Our estimates of argon column in the atmosphere and of argon loss rates are strictly planetwide and daily averages.

We assume that the argon gas diffuses outward to a connected pore space, from which it can reach the surface by Knudsen flow. We assume a fractal distribution of rock sizes, and we assume that the smallest rock size in the distribution increases with depth as illustrated in Fig. 1. For the purpose of this paper, the definition of a rock radius is the shortest distance from the center of the "rock" to a pore space which is connected to the surface *via* pathways that are open either all of the time or at reasonably short time intervals. We show that

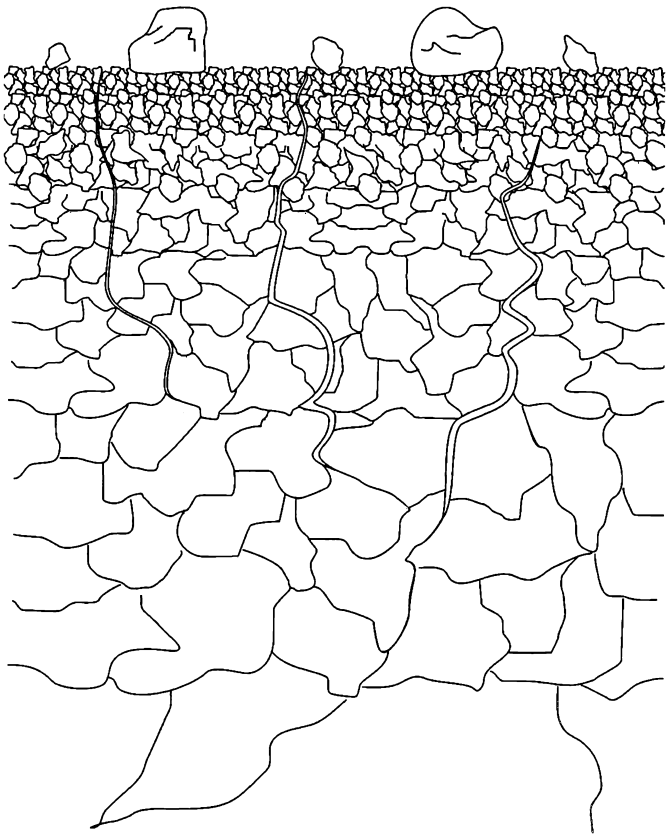

FIG. 1. The distribution of effective rock sizes, illustrated here schematically, is assumed to be fractal with a fractal dimension of 2.5. The smallest unit at the surface is 30 μm. The smallest unit size at depth, z, is 0.003 $z^{0.8}$ (cm), where z is in centimeters. Thus the smallest distance to a connected pore space at a depth of 25 km is 3.9 m.

because the flux to the surface from the "rock unit" depends not only on the temperature and time but also on the rock size, the maximum flux from an ensemble of rock sizes may not correspond to the highest temperature.

^{40}Ar in the atmospheres of the planets is a measure of potassium abundance in the interiors, since ^{40}Ar is a product of radiogenic decay of ^{40}K by electron capture with the subsequent emission of a 1.46 MeV γ-ray. ^{36}Ar is only 1/15 as abundant in the lunar atmosphere as ^{40}Ar, indicating that captured solar wind argon is not a large fraction of the atmospheric argon. We expect it to be even less important at Mercury due to the intrinsic planetary magnetic field. Although the ^{40}Ar in the Earth's atmosphere is expected to have accumulated since the late bombardment, ^{40}Ar in the atmospheres of Mercury and the Moon is eroded quickly by photoionization and electron impact ionization, followed by pick-up by the interplanetary magnetic field. We will assume that 50% of the newly created ions are recycled to the surface (Manka and Michel, 1971), although it has been argued that a larger percentage may be recycled at Mercury (Sarantos, 2002).

First we consider production of ^{40}Ar from ^{40}K, and its diffusion to the surface. It is well known that the noble gases readily diffuse through the rocks in which they are found because of their unique qualities, and diffusion of argon has been well studied (*e.g.*, Mussett, 1969). However, detailed calculations of diffusion of argon through a regolith and megaregolith have not been published previously. We fit the results of numerical calculations of diffusion of argon to the surface of spheres of various sizes to an analytic function so that we can integrate this function over the distribution of radii and over depth. We assume a fractal distribution of effective unit sizes, and we assume that the minimum unit size increases with depth.

Argon was measured on the lunar nightside by the Apollo lunar mass spectrometer package (ALSEP) carried by *Apollo 17* (Hoffman *et al.*, 1973). The dayside measurements were contaminated by outgassing from the Apollo Lander and astronauts, and were not useable. The density of ^{40}Ar at the lunar surface is $<10^2$ at night to 10^5 at the equator at sunrise, with a scale height of ~50 km (Hodges, 1975; Manka and Michel, 1973). The average rate of effusion of ^{40}Ar from the lunar interior was estimated to be between 790 and 1581 atoms cm^{-2} s^{-1} (corresponding to a global average column of (1.3–2.7) $\times$ 10^9 atoms cm^{-2}) with a most probable value of 1154 atoms cm^{-2} s^{-1} (Hodges and Hoffman, 1974). Manka and Michel (1971) estimated that the steady-state surface ^{40}Ar concentration in the lunar atmosphere is about 10^2 to 10^3 cm^{-3}.

The lunar atmospheric argon abundance appears to be consistent with episodic release. Three of the four argon release events observed by the Apollo 17 mass spectrometer were correlated with shallow moonquakes (Hodges and Hoffman, 1974; Hodges, 1977). The global release rates in 1973 were 3.5×10^{21} s^{-1} in February, 6×10^{21} in March, 3.7×10^{21} in June, and 2×10^{21} in August, and appear to be correlated with seismic activity measured by the ALSEP lunar seismic network (Hodges, 1977; Nakamura *et al.*, 1974). These seismic events were given as evidence for an episodic opening of deep fractures or vents in which the argon could be released to the surface. An alternative hypothesis was advanced that time variations in the atmospheric argon were due to release of argon temporarily trapped in lunar cold traps, where ^{40}Ar could be tapped at temperatures <70 K for a year or more at latitudes >75° (Hodges, 1980). Our results are consistent with the proposal that shallow moonquakes release argon (Binder, 1980). Shallow moonquakes redistribute the open pore volume, so that previously open pore space may become closed and new pores may become open to the surface. In this way the upper megaregolith can be degassed.

^{40}Ar escapes from the Moon at a rapid rate: 3–6% of the total ^{40}Ar production rate or 12% of the rate if K is confined to depths <25 km. K should be preferentially placed in the upper crust as a result of early differentiation, resulting in a potassium abundance of 300 < [K] < 600 ppm in the upper 25 km (Taylor and Jakes, 1974). Because at the time there appeared to be little evidence for deep fracturing of the lunar crust, Hodges concluded that ^{40}Ar could not be released from lunar rocks by diffusion, and that a molten source region at great depth was required (Hodges, 1977). Following the measurement of argon in the lunar atmosphere, with global loss rates $<2 \times 10^{21}$ atoms s^{-1} (5269 atoms cm^{-2} s^{-1}), the hypothesis was advanced that radiogenic gases were released from a semi-molten asthenosphere in which they were trapped to depths of 600–1000 km. Hodges (1980) concluded that the source of the atmospheric argon must be localized hot regions. Hodges *et al.* (1973) conclude that this loss rate and the observed time variability requires argon release through seismic activity, tapping a deep argon source. Turcotte and Schubert (1988) postulate that the Moon may be quite porous to this depth.

We propose that the current effusive flux of argon into the atmospheres of Mercury and the Moon is consistent with diffusion from a highly fractured crust, but, contrary to the Hodges' theory outlined above, release from great depth during seismic events is not necessary to maintain the observed atmosphere of the Moon. We believe that episodic release correlated with shallow moonquakes is consistent with a source in the upper 25 km, not at great depth where argon may have been released to an asthenosphere above the closure temperature. The overpressure serves to effectively close pores at greater depths than ~25 km on the Moon (Heiken *et al.*, 1991).

SOURCE PROCESSES

Diffusion

We first train our model to produce the global average argon abundance in the lunar atmosphere. We will examine the possibilities of sustaining an argon atmosphere by diffusion from the upper 10 km of crust, and subsequently by effusion

to the surface. We do not consider redistribution of argon in the atmosphere, condensation at night or freezing out at the poles. These details have been considered for the Moon by Hodges (1975, 1980).

We have used a multipath diffusion code (Lee and Aldama, 1992) to numerically calculate the diffusion of argon from the rocks in which it is created. This multipath diffusion code was written to solve the diffusion equations for a system in which two diffusion paths with different diffusion rates are possible, with an exchange between the two. We are using the code to simulate radiogenic production of ^{40}Ar from ^{40}K, with subsequent diffusion of ^{40}Ar. The diffusion rate for ^{40}K is assumed to be zero, with the exchange rate equal to the radiogenic production rate. We have assumed spherical rock units, the diameter of which is the distance between connected pore spaces. After diffusion to a pore space the argon is assumed to diffuse to the planet's surface by Knudsen flow, a process which is so rapid in comparison with diffusion that it can be assumed to be instantaneous. The diffusion of argon has been reviewed by Mussett (1969). Diffusion rates are very sensitive to temperature, mineral type and physical condition of the mineral. The paths described below do not include the additional path in the connected pore space in which diffusion is characterized by Knudsen flow.

The two-path diffusion equations (Lee and Aldama, 1992) are

$$\frac{\partial \xi}{\partial t} = \nabla\left(D_1 \nabla \xi\right) - K_1 \xi - K_2 \omega \tag{1}$$

$$\frac{\partial \omega}{\partial t} = \nabla\left(D_2 \nabla \omega\right) + K_1 \xi + K_2 \omega \tag{2}$$

where ξ and ω are the concentrations in the low and high diffusivity paths, respectively; ξ = concentration of potassium, ω = concentration of argon, K_1 is the exchange rate of argon and calcium from the potassium cell (*i.e.*, the radiogenic production rate), and K_2 is the exchange rate of potassium to the argon cell: $\xi_o = 1$, $\omega_o = 0$, $D_1 = 0$, $K_2 = 0$. In this case D_1 is zero, which means that potassium does not diffuse out of the cell: the low diffusivity path only contains potassium. The production rate for argon is 0.1048 of the total radiogenic production rate. In this way we allow the source argon atoms to leak out of path 1 at an exchange rate equal to the argon production rate. The potassium is depleted by production of both argon and calcium. The flux per unit volume is scaled by the potassium abundance and total mass density.

Because of uncertainties in mineral type, we will assume that the diffusion coefficient for the lunar regolith is (a) 10^{-19} cm^2 s^{-1}, appropriate for orthoclase at 275 K (extrapolated from measurements by Brandt and Bartnitskiy, 1964), or (b) 10^{-24} cm^2 s^{-1}, appropriate for anorthite at 275 K (from measurements by Fechtig *et al.*, 1960). Because the diffusion coefficients for orthoclase minerals were only measured for temperatures above 400 °C, their extrapolation to 275 K is extremely uncertain. However, we are certain that 10^{-19} cm^2 s^{-1} is an upper limit to the diffusion coefficient for the Moon. That for Mercury is taken as 10^{-15} cm^2 s^{-1}, assuming anorthite at 450 K (Mussett, 1969 after Fechtig *et al.*, 1960). The mineral content of Mercury is undetermined at this time (Cooper *et al.*, 2001).

We assume a fractal distribution of unit sizes, where a unit is a cohesive grain or rock through which the argon must diffuse to reach a connected pore space. The unit may be a grain, a rock or a larger structure. Therefore the diffusion coefficient does not strictly correspond to grain boundary or volume diffusion. However, argon is most likely to reside in the grain boundary region because potassium is an incompatible element. The fractal dimension is assumed to be 2.5 ($dn(r) = (r/r0)^{-2.5}\, dr$), consistent with projectile fragmentation of quartzite or basalt (Turcotte, 1997). The smallest unit at the surface is 30 μm, consistent with the grain size and distribution measured for the lunar regolith (Heiken *et al.*, 1991). The smallest unit increases with depth, z (cm), as $z^{0.8}$. In other words the smallest unit at depth, z, is $r_0(z) = 0.003\, z^{0.8}$ cm.

Results of Diffusion Calculations

We solved for diffusion of radiogenic ^{40}Ar from spherical units of radius, a, given diffusion coefficient, D, using the multipath diffusion code (Lee and Aldama, 1992). These results were validated by comparison with the analytic solution for the ratio of the argon remaining in a sample to the potassium in the sample (Wasserburg, 1954):

$$\frac{^{40}\mathrm{Ar}}{^{40}\mathrm{K}} = \left(\frac{R}{1+R}\right) \times \left[-1 + \left[6\frac{d^2}{\pi^2}\left[\sum_{m=1}^{1000} \frac{\exp\left[x\left[1-\left(m^2\frac{\pi^2}{d^2}\right)\right]\right]}{\left(d^2 - \pi^2 m^2\right)m^2}\right] - 3\frac{\cot(d)}{d} + \frac{3}{d^2}\right]\right] \tag{3}$$

where R is the branching ratio to the production of ^{40}Ar (0.1048), and $d^2 = \lambda a^2/D$. The decay rate, λ, is 7.833×10^{-10} per year, and $x = \lambda t$. We have taken $t = 3.1$ Ga, assuming that diffusion begins after the time of the heavy bombardment. Thus x and d are unitless parameters. The results of Eq. (3) agreed with our numerical solution.

In order to integrate the flux over the size distribution and over depth, we fit the flux of argon per unit volume calculated with the numerical diffusion code to a function, $F(r)$, written as a matrix equation:

$$F(r) = c[S]\left[\frac{1}{1+\exp\left[-\left(\frac{r-\mu}{\alpha}\right)^{\gamma}\right]\left(\frac{r-\mu}{\alpha}\right)^{\frac{\gamma}{2}}}\right]^{\frac{1}{1+r}} \tag{4}$$

TABLE 1. Values for analytic fit to diffusive flux.

log(D)	S1	S2	α	μ	γ
–15	0.255	–20.652	15	0.001	1.0
–19	0.265	–0.634	1.5	0.001	0.6
–24	0.305	–0.201	0.11	0.001	0.52

where $F(r)$ is the argon flux per unit volume from a sphere of radius, r; S is a matrix of constants, μ; α and γ are parameters of a Weibull distribution; and c is the number of ^{40}K atoms cm^{-3} × 10^{-18}. This fit was done using Mathcad. To obtain flux to the surface, we integrated this function over a fractal size distribution of units with fractal dimension 2.5, and over depth to 25 km, where the connected pore space is effectively cut off by pressure (Heiken *et al.*, 1991).

Knudsen flow to the surface in connected pore space is assumed to be instantaneous; our calculations showed it to be orders of magnitude faster than diffusion. The values of matrix [S] and the parameters to Eq. (4) are given in Table 1 for log (D) = –15, –19 and –24, respectively, where D is in cm^2 s^{-1}. This fit is not exclusive to Mercury or the Moon but is only a function of the diffusion coefficient.

The constant, C, is 1.5 × 10^{-3}, the number of ^{40}K atoms cm^{-3} × 10^{-18}. The factor 10^{-18} was not included in the matrix [S] multiplying the flux, $F(x)$. We have used lunar abundance of potassium in the crust, 300 ppm, and a density of 2.6 g cm^{-3}. The results can be scaled to abundance and density values as found for the mercurian crust.

An important parameter is the radius below which negligible flux is obtained. For units smaller than the minimum, the flux at the current time is the current production rate. In other words, very small grains degas so rapidly that the current flux can be assumed to be equal to the current production rate. For this reason the maximum flux will not correspond to the highest temperature. The limiting flux for small units is the current production rate. The flux out as a function of unit size is shown in Fig. 2 for D = 10^{-19} cm^2 s^{-1} and in Fig. 3 for D = 10^{-15} cm^2 s^{-1}. A comparison of Figs. 2 and 3 will help the reader to understand why the diffusive flux is not a monotonic function of D. For small rock units, the flux at the present time may be greater for small values of D than for large values of D because for smaller diffusion rates there is a larger increase in the argon abundance in the rock over time.

The functions, $F(r)$, were integrated over the fractal distribution of unit sizes with fractal dimension 2.5 and over

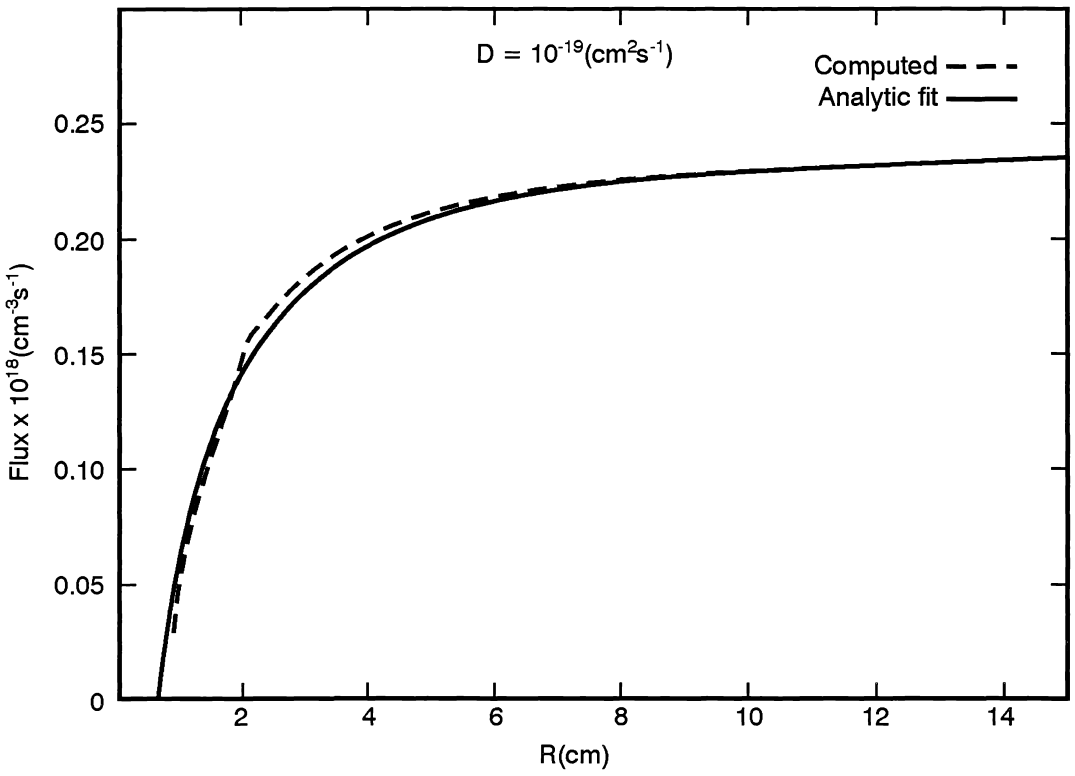

FIG. 2. Flux of argon atoms per unit volume from spheres of radius, R, at 3.1 g year for diffusion coefficient, D = 10^{-19} cm^2 s^{-1}. This diffusion coefficient, measured for orthoclase at 275 K, is within the range of values appropriate for the lunar crust. The flux as computed with the multipath diffusion code is the dashed line, and the analytical fit to these results is the solid line. Without radiogenic production, the curve would resemble a Weibull distribution curve, with a maximum flux at a radius depending on diffusion coefficient and time. With radiogenic production, the curve becomes asymptotic at large radii because argon continues to be produced within the rock.

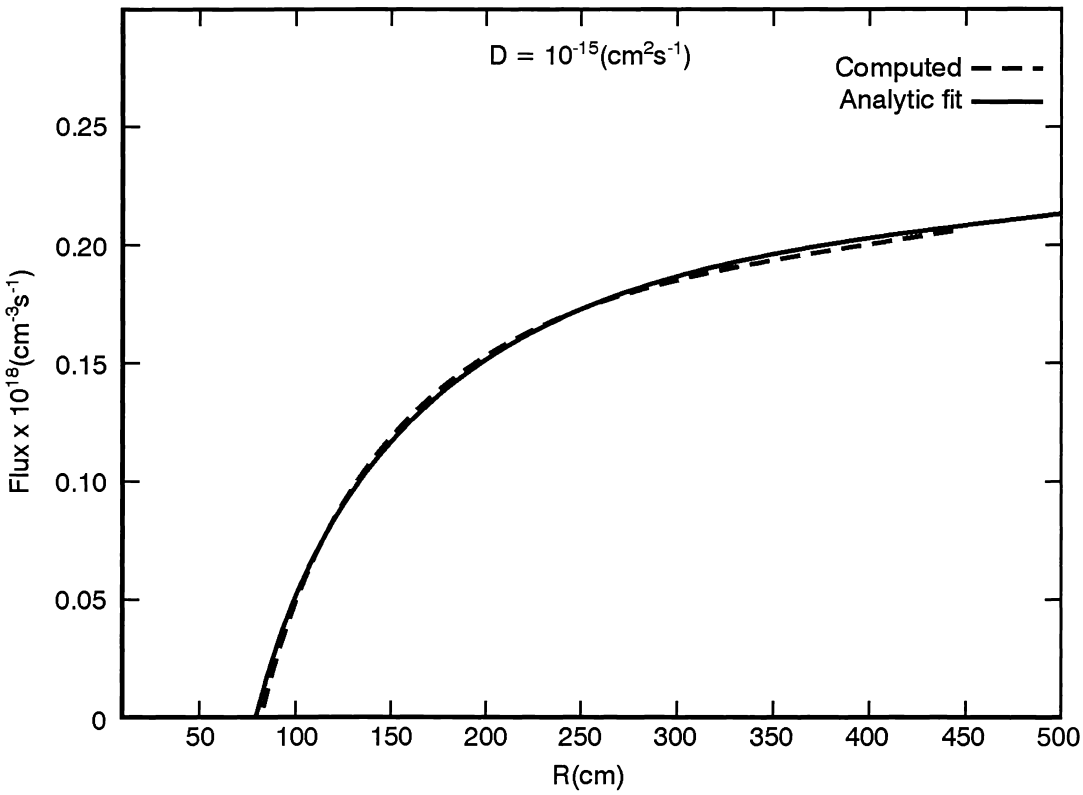

FIG. 3. The same as Fig. 2 for $D = 10^{-15}$ cm^{-2} s^{-1}. This diffusion coefficient, measured for anorthite at 450 K, is assumed to be appropriate for the crust of Mercury.

depth, z, to a depth of 25 km. We assume that the pore spaces are closed below 25 km. Note that if all of the current argon production in the top 25 km were currently being supplied to the surface the flux would be 9019 atoms cm^{-2} s^{-1}.

Moon–Given $x_0(z) = 0.003\ z^{0.8}$ cm, we conclude that the current flux of argon for $D = 10^{-19}$ cm^2 s^{-1} is 990 atoms cm^{-2} s^{-1}, and that for $D = 10^{-24}$ cm^2 s^{-1} is 1448 atoms cm^{-2} s^{-1}. These values are within the limits to the flux estimated to be required by ALSEP measurements of lunar argon (Hodges, 1975), and about one-third of the flux estimated during the lunar seismic event of August 1973. The lunar crustal temperature to 25 km is within the range of values consistent with $-24 < \log(D) < -19$, and the measured atmospheric argon is consistent with the flux derived for diffusion coefficients in this range with a fractal distribution of unit sizes. The flux is not very sensitive to the exact diffusion coefficient in this range for our fractal distribution of sizes because all diffusion regimes give the same limiting flux for very small and very large unit sizes. The flux from very small rock units will be limited by the current production rate. This result is in contrast to that for non-radiogenic elements for which the flux at large times will go to zero for small unit sizes, reach a maximum for some radius, and decline for size units larger than this radius which is a function of time.

Mercury–The measurement of argon in Mercury's atmosphere by *Mariner 10* was inconclusive. An upper limit for the argon abundance in the mercurian atmosphere was obtained by the UVS spectrometer onboard *Mariner 10* (Broadfoot *et al.*, 1976). The subsolar surface abundance of argon is certainly $<6.6 \times 10^6$ cm^{-3} (Shemansky, 1988). Assuming a temperature of 450 K, this gives a column abundance of $<1.6 \times 10^{13}$ cm^{-2} which would imply that Ar may be the most abundant species in the mercurian atmosphere. However, this value is an upper limit based on the sensitivity of the ultraviolet spectrometer (UVS).

Argon is lost from the exosphere by photoionization, followed by entrainment in the solar wind. With a photoionization lifetime at aphelion (0.46 AU) of ~8 days for quiet Sun, or as short as 3.5 days at perihelion (0.306 AU) for active Sun (using rates from Huebner *et al.*, 1992), any argon in the atmosphere would represent current effusion rates. Some argon ions will become entrained in the solar wind, but some will re-impact the surface of the planet. The escape flux of argon ions from Mercury's magnetosphere is an open question since the degree to which the magnetosphere is open to the solar wind is unknown (Luhmann *et al.*, 1998; Kabin *et al.*, 2000; Sarantos *et al.*, 2001; Sarantos, 2002). The fraction of argon ions that escape from Mercury is certainly less than that at the Moon, estimated to be about half the ionization production (Manka and Michel, 1971).

For $D = 10^{-15}$ cm^2 s^{-1}, the current flux to the surface is 1830 atoms cm^{-2} s^{-1}, given the same fractal distribution of

TABLE 2. Argon flux estimated as a function of diffusion coefficient.

log(D)	Flux to the surface (atoms cm^{-2} s^{-1})
−15	1830
−19	990
−24	1448

unit sizes assumed above. In this case 70% of the flux comes from the upper 3.5 km, and corresponds to the current production. These results can be scaled to the K abundance, which we have assumed to be 300 ppm. These results are summarized in Table 2. Note that the flux does not vary monotonically with D because we have assumed a fractal distribution of rock unit sizes and because ^{40}Ar is a radiogenic species. The total flux is given by an integral over the size distribution of rock units and over depth. A comparison of Figs. 2 and 3 illustrates how the flux varies with rock unit size at two different values of D. Because the outgassing at Mercury (D = 10^{-15} cm^2 s^{-1}) is rapid, it is mostly dependent on the potassium abundance, and less dependent on temperature. The argon in the atmosphere will be a direct measure of potassium abundance in the crust.

In contrast with the Moon, the lifetime of argon at Mercury is only ~3.5 days at perihelion or 8 days at aphelion, giving a total column abundance of about 5×10^8 to 1.2×10^9 atoms cm^{-2} if the flux is 1830 atoms cm^{-2} s^{-1} (Table 2). This is considerably less than the upper limit given by the *Mariner 10* ultraviolet (UV) spectrometer results. Recycling of half of the argon ions would only increase the above estimates by 20% if equilibrium has been reached at the surface (appendix B).

Effusion

Argon easily escapes from a melt, and would become trapped in pockets, from which it could effuse to the surface if cracks open. Chemical decomposition and melting are important at high temperature (Mussett, 1969). The closure temperature (the apparent temperature at which Ar is retained in a laboratory sample) for K-Ar in K-feldspar is 440–640 K (Lovera *et al.*, 1989; Hodges, 1991), within the range expected for the regolith and upper crust of Mercury. However, the upper 100 km of the Moon is expected to be under 350 K, and will be below the closure temperature. A wide range of closure temperatures is indicative of multiple diffusion domains, also discussed above.

The thrust faults causing active moonquakes have a depth of 300 m to 3.5 km (Binder, 1980) and thus would episodically connect open pore space to the surface. The argon having diffused out of the crystalline lattice or grain boundary regions into pore spaces would be released episodically to the surface through effusive flow, which is instantaneous on timescales of interest here. Although grinding and melting directly adjacent to the fault will release argon directly from the rock, fracturing of large volumes of rock farther from the fault itself will release significant amounts of ^{40}Ar. It is this process which is important in opening the connected pore spaces and releasing argon which is already in pore spaces and voids.

ATMOSPHERIC ESCAPE

Argon is gravitationally bound on both Mercury and the Moon, and ionization losses dominate over Jeans escape. Argon atoms are mainly lost by photoionization and secondarily by electron impact ionization. At the Moon about half of these ions will return to the surface, where most will become implanted (Manka and Michel, 1971). First, we look at the effect of ion implantation on the net flux of argon from the crust and regolith. We assume that the argon ions are implanted into rock units of radius, a. In the following discussion we assume that the implantation can be treated as a source in a similar way as the radiogenic source, but with a different source rate given by the implantation rate.

The number of argon atoms in a sphere of radius, a, with volume, V, at quasi-equilibrium with a concentration of ^{40}K, C_K, is (Mussett, 1969)

$$n = \frac{V \times \lambda \times C_K \times a^2}{15D} \tag{5}$$

where λ is the radiogenic decay rate of ^{40}K, and D is the diffusion coefficient. If we substitute for λC_K a constant source S (cm^{-3} s^{-1}), we have an equilibrium concentration, ns of

$$ns = \frac{S}{15} \times \frac{a^2}{D} \tag{6}$$

We assume initially that S is half of the ionization flux. Now solving for the loss of argon by diffusion from a sphere with an equilibrium concentration, ns, we obtain a loss rate of 6/15 the incoming flux. Thus the global flux of neutrals to the atmosphere is the outgassing flux from the interior plus 3/15 of this flux, or a factor of 1.2 of the effusion rate from the interior. The rate of trapping of ^{40}Ar in the lunar rocks was estimated by Heymann and Yaniv (1970) to be 400 atoms cm^{-2} s^{-1}. If this represents half of the ion loss rate, then the ion loss rate is 800 cm^{-2} s^{-1}, consistent with the lower limit of the effusive flux estimated by Hodges and Hoffman (1974). In reality, only a fraction of the returning ions will be trapped in the grains, so these results are fully consistent.

Argon is lost from the atmosphere by photoionization and by electron impact ionization. The primary loss mechanism at both Mercury and the Moon is photoionization. At Mercury, electron impact ionization is more important than at the Moon, but still less important than photoionization. The photoionization rate for argon at Earth orbit is given by Huebner *et al.* (1992) as 3.05×10^{-7} s^{-1} for quiet Sun and 6.9×10^{-7} s^{-1} for active Sun. This gives a lifetime against ionization at the

Moon of 38 days for quiet Sun, and 17 days for active Sun. The value used to analyze the lunar ALSEP data was 18 days (Manka, 1973), but this is probably too short based on the mean monthly sunspot number at the time. For this analysis we will use an ionization lifetime for Ar at the Moon as 23 days, midway between quiet and active Sun conditions. Adding an additional 14 days for nighttime, during which the argon is sequestered in the soil, the lifetime is 37 days. This is reasonably consistent with the lifetime derived by Hodges: 50 days. Using a time average, the effusion rate of new argon atoms is equal to the photoionization rate minus 6/15 of the rate of return of photoions to the surface. Thus the effusion rate is 80% of the photoionization rate if half of the photoions return to the surface as calculated by Manka and Michel (1971).

Assuming that the lifetime of argon in the lunar atmosphere is 37 days, 23 days for photoionization plus 14 days spent on the nightside, the average total column of ^{40}Ar would be 4.6×10^9 cm^{-2}. The lunar average degassing rate required by the Apollo 17 lunar surface mass-spectrometer results with no recycling of ions is 2×10^{21} atoms s^{-1}. The mean photorate at Mercury mean orbit is $2.94 \times 10^{-6}/2$ s^{-1}, taking into account the time in darkness. Thus the lifetime of an argon atom in Mercury's atmosphere would be 7.9 days. Argon atoms diffusing into the atmosphere during nighttime would be subject to electron impact ionization, with a lifetime of ~89.7 days. On average the argon would persist in the atmosphere until rotated into the sunlight. The lifetime of argon in the lunar atmosphere is between 16.8 (active Sun) and 38.6 days (quiet Sun), plus 14 days in darkness. The lifetime of an argon atom in the lunar atmosphere during the ALSEP program was ~37 days. If the flux out of Mercury's crust is 1830 atoms cm^{-2} s^{-1} (Table 2) and the lifetime is 7.9 days, the average column abundance would be 1.3×10^9 cm^{-2}, roughly comparable to the lunar column abundance.

CONCLUSIONS

We expect the atmospheric argon abundance at Mercury to be less than or comparable to that at the Moon. This is in sharp contrast with the sodium and potassium atmospheres of the two bodies, where the mercurian abundance of sodium is 2 orders of magnitude greater than that at the Moon. This results from differences in the source processes of the alkalis and the rare gases. Killen *et al.* (2001) and McGrath *et al.* (1986) argued that the former are probably preferentially derived from the surface by photon-stimulated desorption which increases as the inverse square distance from the Sun, although evaporation (Sprague, 1990), ion sputtering (Potter and Morgan, 1990), and meteoritic vaporization (Cintala, 1992; Killen *et al.*, 2001) also play important roles. The means of replenishing the surface with a fresh supply of alkalis has been debated in the literature. Whereas Sprague (1990) has argued that the alkalis are brought to the surface by diffusion, Killen and Morgan (1993a,b) have argued that diffusion of the alkalis is inefficient, and that meteoritic gardening is sufficient. In contrast, argon, being a noble gas, easily diffuses through a rock (*e.g.*, Mussett, 1969), and readily evaporates at the surface (Hodges, 1975, 1977; Hodges *et al.*, 1973).

Although the diffusion coefficients depend exponentially on temperature, the effusive flux is limited by the radiogenic production rate and by the distance between connected pore space. These parameters have been assumed to be fractal. For a non-radiogenic species, there will be a pulse of diffusant at the surface of a given size grain or unit at a given time after solidification. For a radiogenic diffusant, there is an asymptotic value of the diffusive flux for large rock sizes. For a fractal distribution, then, at a given time a different size of grain or unit will be the major source of gas to the pore space. For two very different diffusion regimes a different size unit will dominate the source at a given time. If many size units are all available, the diffusant is radiogenic and the parent is uniformly distributed, the flux out of the crust will depend less on temperature (diffusion coefficient) and more on the distribution of unit sizes. Loss rates from the atmosphere are much larger at Mercury than at the Moon because photoionization loss dominates. Even though the ion recycling rate may be much larger at Mercury than at the Moon, this will not alter our results by more than a factor of 2.

In future work, we will consider how the mercurian magnetosphere affects the loss of argon. Because argon is both heavy and accommodated to the surface temperature, its scale height will be much smaller than the distance to the magnetopause. It is important to model this effect on the argon loss rate in order to understand measurements of atmospheric argon.

Acknowledgements–The author was supported by the NASA Planetary Atmospheres Program under grant NAG5-6998. We thank two anonymous referees for suggestions that greatly improved the manuscript.

Editorial handling: S. R. Taylor

REFERENCES

BINDER A. B. (1980) Shallow Moonquakes: Argon release mechanism. *Geophys. Res. Lett.* **7**, 1011–1013.

BRANDT S. B. AND BARTNITSKIY E. N. (1964) Losses of radiogenic argon in potassium-sodium feldspars on heat activation. *Int. Geol. Rev.* **6**, 1483–1489.

BROADFOOT A. L., SHEMANSKY D. E. AND KUMAR S. (1976) Mariner 10—Mercury atmosphere. *Geophys. Res. Lett.* **3**, 577–580.

CINTALA M. J. (1992) Impact-induced thermal effects in the lunar and mercurian regoliths. *J. Geophys. Res.* **97**, 947–973.

COOPER B., POTTER A. E., KILLEN R. AND MORGAN T. (2001) Midinfrared spectra of Mercury. *J. Geophys. Res.* **106**, 32 803–32 814.

FECHTIG H., GENTNER W. AND ZAHRINGER J. (1960) Argonbestimmungen an Kalium-mineralien–VII. Diffusionrverluste von argon mineralien und ihre auswirkung aud die kalium-argon-alterbestimmung. *Geochim. Cosmochim. Acta* **19**, 70–79.

HEIKEN G. H., VANIMAN D. T. AND FRENCH B. M. (1991) *Lunar Sourcebook*. Cambridge Univ. Press, Cambridge, England. 736 pp.

HEYMANN D. AND YANIV A. (1970) ^{40}Ar anomaly in lunar samples from Apollo 11. *Proc. Lunar Sci. Conf.* 1261–1267.

HODGES R. R., JR. (1975) Formation of the lunar atmosphere. *The Moon* **14**, 139–157.
HODGES R. R., JR. (1977) Release of radiogenic gases from the Moon. *Physics Earth Planet. Sci. Interiors* **14**, 282–288.
HODGES R. R., JR. (1980) Lunar cold traps and their influence on argon-40. *Proc. Lunar Planet. Sci. Conf.* **11th**, 2463–2477.
HODGES R. R., JR. (1991) Exospheric transport restrictions on water ice in lunar polar traps. *Geophys. Res. Lett.* **18**, 2113–2116.
HODGES R. R., JR. AND HOFFMAN J. H. (1974) Episodic release of ^{40}Ar from the interior of the Moon. *Proc. Lunar Sci. Conf.* **5th**, *Geochim. Cosmochim. Acta* **3**, 2955–2961.
HODGES R. R., JR., HOFFMAN J. H., JOHNSON F. S. AND EVANS D. E. (1973) Composition and dynamics of lunar atmosphere. *Proc. Lunar Sci. Conf.* **4th**, *Geochim. Cosmochim. Acta* **3 (Suppl.)**, 2855–2864.
HOFFMAN J. H., HODGES R. R., JOHNSON F. S. AND EVANS D. E. (1973) Lunar atmospheric composition results from Apollo 17. *Proc. Lunar Sci. Conf.* **4th**, *Geochim. Cosmochim. Acta* **3 (Suppl.)**, 2865–2875.
HUEBNER W. F., KEADY J. J. AND LYON S. P. (1992) Solar photo rates for planetary atmospheres and atmospheric pollutants. *Astrophys. Space Sci.* **195**, 1–294.
KABIN K., GOMBOSI T. I., DEZEEUW D. L. AND POWELL K. G. (2000) Interaction of Mercury with the solar wind. *Icarus* **143**, 397– 406.
KILLEN R. M. AND MORGAN T. H. (1993a) Diffusion of Na and K in the uppermost regolith of Mercury. *J. Geophys. Res.* **98**, 23 589–23 601.
KILLEN R.M. AND MORGAN T. H. (1993b) Maintaining the Na atmosphere of Mercury. *Icarus* **101**, 293–312.
KILLEN R. M., POTTER A. E., REIFF P., SARANTOS M., JACKSON B.V., HICK P. AND GILES B. (2001) Evidence for space weather at Mercury. *J. Geophys. Res., Planets* **106**, 20 509–20 525.
LEE J. K. W. AND ALDAMA A. A. (1992) Multipath diffusion: A general numerical model. *Comp. Geosci.* **18**, 531–555.
LOVERA O. M., RICHTER F. M. AND HARRISON T. M. (1989) ^{40}Ar/^{39}Ar geothermometry for slowly cooled samples having a distribution of diffusion domain size. *J. Geophys. Res.* **94**, 17 917–17 936.
LUHMANN J. G., RUSSELL C. T. AND TSYGANENKO N. A. (1998) Disturbances in Mercury's magnetosphere: Are the Mariner 10 "substorms" simply driven? *J. Geophys. Res.* **103**, 9113–9119.
MANKA R. H. (1973) Plasma and potential at the lunar surface. In *Photon and Particle Interactions with Surfaces in Space* (ed. R. J. L. Grard), p. 347. D. Reidel, Dordrecht, Holland.
MANKA R. H. AND MICHEL F. C. (1971) Lunar atmosphere as a source of lunar surface elements. *Proc. Lunar Sci. Conf.* **2nd**, *Geochim. Cosmochim. Acta* **2 (Suppl.)**, 1717–1728.
MANKA R. H. AND MICHEL F. C. (1973) Lunar ion flux and energy. In *Photon and Particle Interactions with Surfaces in Space* (ed. R. J. L. Grard), pp. 429–442. D. Reidel, Dordrecht, Holland.
MCGRATH M. A., JOHNSON R. E. AND LANZEROTTI L. J. (1986) Sputtering of sodium on the planet Mercury. *Nature* **323**, 694–696.
MUSSETT A. E. (1969) Diffusion measurements and potassium-argon method of dating. *Geophys. J. Roy. Astron. Soc.* **18**, 257–303.
NAKAMURA Y., DORMAN J., DUENNEBIER F., EWING M., LANMLEIN D. AND LATHAM G. (1974) High frequency lunar teleseismic events. *Proc. Lunar Sci. Conf.* **5th**, *Geochim. Cosmochim. Acta* **3**, 2883–2890.
POTTER A. E. AND MORGAN T. H. (1990) Evidence for magnetospheric effects on the sodium atmosphere of Mercury. *Science* **248**, 835–838.
RAPP D. AND ENGLANDER-GOLDEN P. (1965) Total cross sections for ionization and attachment in gases by electron impact. I. Positive ionization. *J. Chem. Phys.* **43**, 1464–1479.
RUSSELL C. T., BAKER D. N. AND SLAVIN J. A. (1988) The magnetosphere of Mercury. In *Mercury* (eds. F. Vilas, C. Chapman and M. S. Matthews), pp. 514–561. Univ. Arizona Press, Tucson, Arizona, USA.
SARANTOS M. (2002) A model for magnetosphere-exosphere interaction at Mercury. Ph.D. thesis, Rice University, Houston, Texas, USA.
SARANTOS M., REIFF P. H., HILL T. W., KILLEN R. M. AND URQUHART A. L. (2001) A B_x interconnected magnetosphere model for Mercury. *Planet. Space Sci.* **49**, 1629–1635.
SHEMANSKY D. E. (1988) Revised atmospheric species abundances at Mercury: The debacle of bad g values. *Mercury Messenger* **2**, 1.
SPRAGUE A. L. (1990) A diffusion source for sodium and potassium in the atmospheres of Mercury and the Moon. *Icarus* **84**, 93–105.
TAYLOR S. R. AND JAKES P. (1974) The geochemical evolution of the Moon. *Proc. Lunar Sci. Conf.* **5th**, *Geochim. Cosmochim. Acta* **3**, 1287–1305.
TURCOTTE D. L. (1997) *Fractals and Chaos in Geology and Geophysics*. Cambridge Univ. Press, Cambridge, U.K. 221 pp.
TURCOTTE D. L. AND SCHUBERT G. (1988) Tectonic implications of radiogenic noble gases in planetary atmospheres. *Icarus* **74**, 36–46.
WASSERBURG G. J. (1954) ^{40}Ar-^{40}K dating. In *Nuclear Geology* (ed. H. Faul), pp. 341–349. Wiley, New York, New York, USA.

APPENDICES

APPENDIX A

The flux of argon diffusing out of the regolith at time, t, for $D = 10^{-19}$ cm^2 s^{-1} is given by:

$$\text{frac} = \int_{1.25\times10^3}^{2.5\times10^6}\int_{1}^{300}\left[\left[(0.265)\times\left[1+\exp\left[-\left[\frac{\left(0.003\times z^{0.8}\times a\right)-\mu}{\alpha}\right]^{\gamma}\right]\times\left[\frac{\left(x0(z)\times a-\mu\right)}{\alpha}\right]^{\frac{\gamma}{2}}\right]\right]-\frac{0.634}{1+0.003\times z^{0.8}\times a}\right]\times\frac{(a)^{-2.5}}{0.666667}\,da\,dz \quad \text{(A.1)}$$

assuming that the minimum radius at depth, z, is $r_0 = 0.003\ z^{0.8}$ cm, the size distribution at a given depth, z, is $f(r) = (r/r0)^{-2.5}$, and the flux is 1.456×10^{-3} frac (cm^{-2} s^{-1}). The limits on z are in centimeters, and a is a unitless radius. The integration limits on z are given in centimeters, and a is a unitless parameter. The constants α, γ, and μ are given in Table A1. The constant equal to 1.45×10^{-3} is the total number of ^{40}K atoms per unit volume, assuming a density of 2.6 g cm^{-3}, and a lunar crustal K abundance of 300 ppm and the scale factor 10^{-18}, which was not included in frac for plotting purposes. The results can be scaled to the K abundance and the density.

TABLE A1. Parameters for analytical fit to diffusive flux.

log(D)	α	γ	μ
–15	15.0	1.0	0.001
–19	1.5	0.6	0.001
–24	0.11	0.52	0.001

APPENDIX B

The Electron Impact Ionization Rate at Mercury

In order to determine the electron impact loss rate at Mercury we fit the electron impact cross section, $\sigma(E)$, as a function of energy, E (keV), given by Rapp and Englander-Golden (1965) to a function, $F(x)$. We integrated this function over the electron energy at Mercury given by Russell *et al.* (1988).

$$F1(E) = \begin{bmatrix} \exp[-(1+3.5\times E)] \\ \dfrac{1}{(4\times E)^3} \\ 1+\exp\left[-(3.7\times E)^2\right] \\ \cos(3.2E) \end{bmatrix} \quad \text{(A2.1)}$$

$$S = \begin{pmatrix} -9.676 \\ -4.416\times 10^{-4} \\ 1.567 \\ 0.443 \end{pmatrix} \quad \text{(A2.2)}$$

The cross section is given by

$$\sigma(E) = -9.676\exp[-1+35\times E)] + 0.433\times\cos(3.2\times E) + 1.567\times\left[1+\exp[-(3.7\times E)^2]\right] + \frac{4.416\times 10^{-4}}{(4\times E)^3} \quad \text{(A2.3)}$$

where σ is in barns (the area of the hydrogen nucleus).

The electron flux (particles $cm^{-2}\ s^{-1}\ sr^{-1}\ keV^{-1}$) as a function of energy in keV (Russell *et al.*, 1988) is fit to

$$F2(E) = 9.17\times 10^{13} + 1.73\times 10^{9}\times \left(1+\frac{1}{E}\right) - \left[\frac{\left(9.184\times 10^{13}\right)}{\left[1+\left(\frac{E}{2}\right)^2\right]}\right] \quad \text{(A2.4)}$$

for photoelectrons of energy $0.01 < E < 0.03$ keV, and

$$F3(E) = -5.399\times 10^{10} - 1.933\times 10^{11}\times\exp(-E) + \frac{2.082\times 10^{11}}{(1+E)} + \frac{\left[4.052\times 10^{10}\right]}{(1+E^2)} \quad \text{(A2.5)}$$

for "cool" electrons of energy $0.03 < E < 0.8$ keV. The electron impact ionization rate was found by integrating

$$ni = \int_{0.015}^{0.03} 2\pi\times 0.001\times F2(E)dE + \int_{0.03}^{0.8} 2\pi\times nar\times\sigma(E)\times F3(E)dE \quad \text{(A2.6)}$$

where the electron impact cross section is taken as a constant near threshold. The resulting loss rate for electron-impact ionization at Mercury is $1.29\times 10^{-7}\ N\ s^{-1}$, where N is the argon column (cm^{-2}).